ELSEVIER

Global left ventricular strains and left atrial volumes are not associated in healthy adults – Detailed analysis from the three-dimensional speckle-tracking echocardiographic MAGYAR-Healthy Study

Attila Nemes [1,*], Árpád Kormányos, Nóra Ambrus, Csaba Lengyel

Department of Medicine, Albert Szent-Györgyi Medical School, University of Szeged, Szeged, Hungary

A B S T R A C T

Introduction: During the heart cycle, left ventricular (LV) contractility is characterized by complex deformation and rotational mechanics, resulting in LV ejection. The present study seeks to expand our knowledge by examining dependence of LV strains representing LV deformation on left atrial (LA) volumes in healthy circumstances. Therefore, the aim of this study was to evaluate the associations between LA volumes and LV strains as assessed simultaneously by three-dimensional speckle-tracking echocardiography (3DSTE) in normal healthy adults.
Methods: The present study consisted of 302 healthy adults, but according to exclusion criteria, 137 subjects were excluded due to inferior image quality. The final population comprised 165 individuals (mean age: 33.1 ± 12.3 years, 75 males) who were voluntarily recruited for screening. Two-dimensional echocardiography extended with 3DSTE was performed in all subjects for detailed LV/LA analysis.
Results: Overall feasibility for simultaneous assessment of LV strains and LA volumes proved to be 55 % with excellent intra- and interobserver correlations. All global LV strains were similar, regardless of the LA volumes examined. All LA volumes and volume-based functional properties respecting the cardiac cycle were similar, regardless the global LV strains examined.
Conclusions: LV strains and LA volumes can be simultaneously assessed by 3DSTE. Global LV strains and LA volumes are not associated in healthy adults.

1. Introduction

Three-dimensional (3D) speckle-tracking echocardiography (3DSTE) can be considered one of the most modern, easy-to-perform, non-invasive cardiovascular imaging procedures suitable for simultaneous quantification of heart chambers [1–6]. It can be used to perform physiological studies to investigate the interaction of certain heart chambers, e.g. LV functional dependence on LV volumes [7]. During the heart cycle, motion of the LV is characterized by a complex deformation and rotational mechanics, resulting in optimal LV ejection [8–11]. In a recent clinical study, strong relations were found between 3DSTE-derived left atrial (LA) volumes throughout the heart cycle and LV rotational mechanics in healthy adults [12]. The present study seeks to expand this knowledge by examining the LA dependence of LV strains,

parameters characterizing LV contractility in healthy circumstances [9–11]. Therefore, the aim of this study was to investigate the associations between LA volumes and LV contractility represented by LV strains in normal healthy adults in a way that all these volumetric and strain parameters were assessed within the same 3DSTE examination.

2. Subjects and methods

2.1. Subjects

The study comprised 302 healthy individuals, from which 137 subjects were excluded due to inferior quality of images. The remaining population comprised 165 individuals (mean age: 33.1 ± 12.3 years, 75 males) who were voluntarily recruited for screening. All tests were

---

performed at the same time between 2011 and 2015 including physical examination, laboratory tests, standard 12-lead electrocardiography and two-dimensional (2D) Doppler echocardiography. Results proved to be within the normal reference range in all subjects. No healthy individuals had any known diseases or (patho)physiological states that could have any effects on the results. No one had taken any medications or drugs. All echocardiographic studies were performed simultaneously, with 3DSTE-based data acquisition performed in conjunction with 2D echocardiographic studies. Detailed offline 3DSTE-based data analysis was performed at a later date. The present retrospective study serves as part of the '**M**otion **A**nalysis of the heart and **G**reat vessels b**Y** three-dimension**A**l speckle-t**R**acking echocardiography in **Healthy** subjects' **(MAGYAR-Healthy) Study**. Among others, this study aimed to perform physiologic studies to determine associations between 3DSTE-derived LV and LA volumetric and functional parameters ('Magyar' means 'Hungarian' in Hungarian language). The Institutional and Regional Human Biomedical Research Committee of University of Szeged, Hungary (No.: 71/2011) approved the study, which was conducted in accordance with the Declaration of Helsinki, all participators gave informed consent.

2.2. 2D Doppler echocardiography

In all healthy subjects, a Toshiba Artida^{TM} echocardiographic device (Toshiba Medical Systems, Tokyo, Japan) attached to a PST-30BT (1–5 MHz) phased-array transducer was used. Routine 2D echocardiographic examination was performed in accordance with the protocol, the dimensions of LA and LV were determined, and the Simpson's method was used for determination of LV ejection fraction (EF). Significant valvular stenoses and regurgitations on any valves were excluded by Doppler echocardiography and mitral inflow velocities measured in diastole and their ratio (E/A) were determined [13].

2.3. 3DSTE

A full-scale 3DSTE study consisted of two parts: first data acquisition was completed, followed by the measurement phase. The same Toshiba Artida^{TM} echocardiography device (Toshiba Medical Systems, Tokyo, Japan) was used in the studies, which was attached to a PST-25SX matrix-array transducer. The subject lying in her/his left side was asked to hold her/his breath, and then data was collected from the apical window with the individual being in sinus rhythm. To achieve optimal image quality, 6 subvolumes were collected within 6 heart cycles, which were automatically merged into a full volume dataset. All offline analyses were performed using the same vendor-provided 3D Wall Motion Tracking software version 2.7 (Ultra Extend, Toshiba Medical Systems, Tokyo, Japan) [1–6].

2.4. 3DSTE-derived LV deformation analysis

From the acquired 3D echocardiographic dataset focused on the LV, optimal apical longitudinal views were selected in apical 4-chamber (AP4CH) and 2-chamber (AP2CH) views and basal, midventricular and apical cross-sectional views. Then septal and lateral mitral annular (MA)-LV edges and endocardial surface of the LV apex were defined and a sequential analysis was started. Finally, a virtual 3D LV cast was created and simultaneous LV volumetric and strain analysis was performed. For LV segmental analysis the 16-segment LV model was used. In each segment, three unidirectional/unidimensional strain parameters were assessed: radial (RS) (thickening and thinning of a segment), longitudinal (LS) (lengthening and shortening of a segment) and circumferential (CS) (widening and narrowing of a segment). Based on these unidirectional/unidimensional strains, complex/multidimensional/ multidirectional strains were also calculated: area (AS) (combination of LS and CS) and 3D (3DS) (combination of RS, LS and CS). Global LV strains were measured describing the whole LV [7] (Fig. 1).

2.5. 3DSTE-derived LA volumetric measurements

Similarly to LV measurements, the LA was assessed on LA-focused images. Firstly, in AP4CH and AP2CH views and 3 short-axis views in basal, midatrial, and superior regions were selected for LA assessments. Later, several reference points were traced around the LA from the lateral MA-LA edge towards the apex of the LA and the septal MA-LA edge. LA appendage and pulmonary veins were not included in the measurements. Finally, a sequential analysis was used to create the virtual 3D LA model, with which the following LA volumes were calculated according to the cardiac cycle (Fig. 2) [12,14]:

- V_{max} – end-systolic maximum LA volume, just before the mitral valve open,
- V_{preA} – LA volume before atrial contraction, at time of P wave on electrocardiogram,
- V_{min} – end-diastolic minimum LA volume, just before the mitral valve close.

Using these LA volumes the following LA volume-based functional parameters were calculated [12,14]:

2.5.1. End-systolic reservoir LA function

- TASV – LA total stroke volume (SV), calculated by V_{max}- V_{min}
- TAEF – LA total emptying fraction, calculated by total SV/V_{max}

2.5.2. Early diastolic conduit LA function

- PASV – LA passive stroke volume, calculated by V_{max}- V_{preA}
- PAEF – LA passive emptying fraction, calculated by passive SV/V_{max}

2.5.3. Late diastolic booster pump (active contraction) LA function

- AASV – LA active stroke volume, calculated by V_{preA}– V_{min}
- AAEF – LA active emptying fraction, calculated by active SV/V_{preA}

2.6. Statistical analysis

The continuous and categorical variables obtained during analyses were displayed as mean ± standard deviation or in number/percent format. $p < 0.05$ was considered to be statistically significant. Fischer's exact test was used for analysis of categorical variables. The normally distributed continuous datasets were analyzed using Student's *t*-test, and in case of non-normal distribution, Mann-Whitney-Wilcoxon test was used. One-way analysis of variance test with Bonferroni correction were used, where appropriate. Intraobserver and interobserver reproducibility was assessed by calculation the intraclass correlation coefficient. All statistical analyses were performed using SPSS software (SPSS Inc, Chicago, IL, USA).

3. Results

3.1. Clinical and 2D Doppler echocardiographic data

From routine 2D echocardiographic data, LA diameter measured in parasternal long-axis view (36.7 ± 4.0 mm), LV end-diastolic diameter (48.1 ± 3.7 mm) and volume (106.9 ± 23.0 ml), LV end-systolic diameter (32.0 ± 3.3 mm) and volume (36.6 ± 9.3 ml), interventricular septum (9.0 ± 1.6 mm) and LV posterior wall (9.1 ± 1.6 mm) and LV-EF (65.8 ± 4.9 %) were in the normal range. Mean E/A proved to be (1.35 ± 0.31). None of the healthy adults showed larger than grade 1 valvular regurgitation or valvular stenosis on any valves.
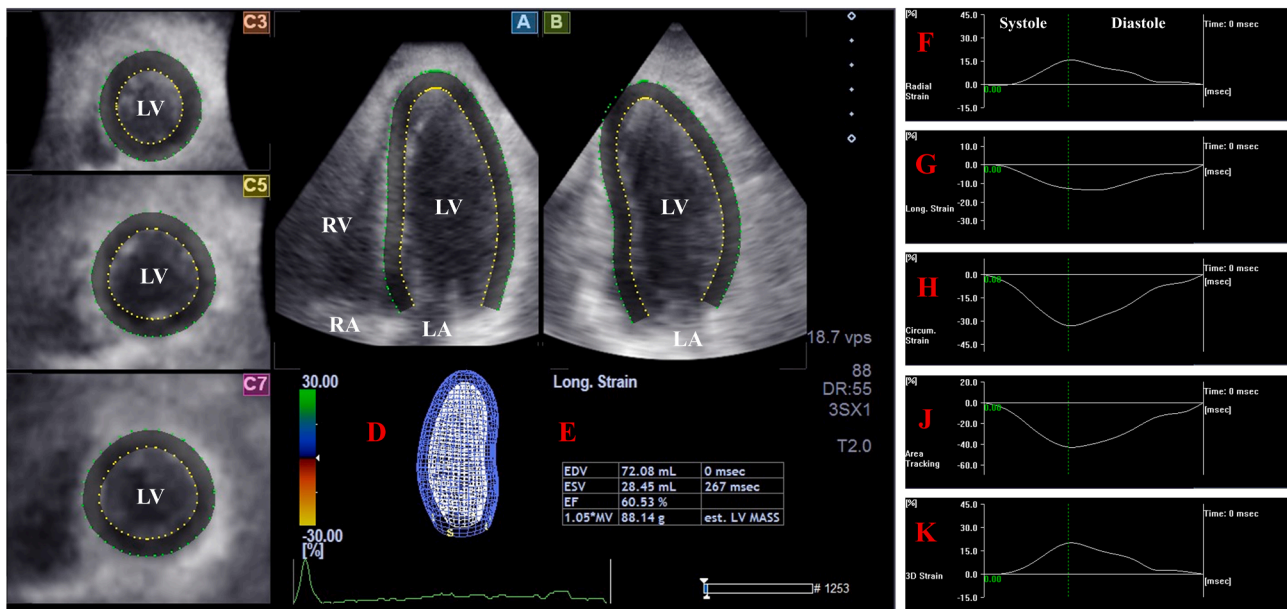
Fig. 1. Three-dimensional (3D) speckle-tracking echocardiographic analysis of left ventricular (LV) strains: apical four-chamber (A) and two-chamber (B) longitudinal views, and basal (C3), mid-ventricular (C5) and apical (C7) short-axis views, which can be automatically extracted from the acquired 3D echocardiography database. Virtual 3D LV cast (D) and volumes and ejection fraction (E) are also presented. Time – global LV radial (F), longitudinal (G), circumferential (H), area (J) and 3D (K) strain curves are also demonstrated (white lines). **Abbreviations:** LA, left atrium; LV, left ventricle; RA, right atrium; RV, right ventricle; EDV, end-diastolic volume; ESV, end-systolic volume; EF, ejection fraction.

3.2. Classification of healthy individuals

Mean ± standard deviation of 3DSTE-derived LA volumes and volume-based functional properties and LV strains of healthy cases are presented in Table 1. Healthy subjects were classified into 3 groups according to the normal LA-V_{max}, LA-V_{preA} and LA-V_{min} and global LV-RS (LV-GRS), LV-CS (LV-GCS), LV-LS (LV-GLS), LS-3DS (LV-G3DS) and LV-AS (LV-GAS): estimated mean ± standard deviation served as the lower (27.8 ml, 15.9 ml, 11.2 ml, 16.1 %, −13.8 %, −22.5 %, 19.0 % and −35.3 %, respectively) and upper (54.0 ml, 39.5 ml, 27.6 ml, 34.9 %, −18.6 %, −32.7 %, 37.2 % and −45.3 %, respectively) values.

3.3. Associations of different LA volumes and volume-based functional properties

Increase of Vmax was associated with increase of VpreA, Vmin and all stroke volumes with preserved TAEF, reduced PAEF and increased AAEF. Increase of VpreA was associated with increase of Vmax, Vmin, TASV and AASV with preserved PASV and reduced TAEF and PAEF. The highest AAEF was detected at the highest VpreA. Vmin was similarly associated with atrial volumes, stroke volumes, and emptying fractions except for AAEF, which showed reduction (Table 2).

3.4. Associations of different LV strains

Increase of LV-GRS, LV-GCS and LV-G3DS was associated with increase of all global LV strains except for LV-GLS. Increase of LV-GAS was associated with increase of all global LV strains. Increase of LV-GLS was associated with simultaneous increase of LV-GAS and LV-GCS and LV-G3DS were the highest, when LV-GLS was the highest (Tables 3–4).

3.5. Different LA volumes and LV strains

All global LV strains were similar, regardless the LA volumes examined (Table 2).

3.6. Different LV strains and LA volumes

All LA volumes and volume-based functional properties respecting the cardiac cycle were similar, regardless of the global LV strains examined (Tables 3–4).

3.7. Feasibility of 3DSTE-derived parameters

All evaluations were performed several times in all individuals, and if findings were found to be consequent, they have been accepted. Adequate simultaneous LA volumetric and LV strain assessments could be performed in 165 out of 302 assessments (55 % overall feasibility).

3.8. Reproducibility of 3DSTE-derived parameters

Intraobserver intraclass correlation coefficients for LA-Vmax, LA-VpreA, LA-Vmin, LV-GRS, LV-GCS, LV-GLS, LS-G3DS and LV-GAS proved to be 0.97, 0.97, 0.89, 0.80, 0.80, 0.82, and 0.82, respectively. Interobserver intraclass correlation coefficients for the same parameters were 0.98, 0.97, 0.88, 0.79, 0.80, 0.80, and 0.78, respectively.

4. Discussion

To the best of authors' knowledge this is the first time to demonstrate that simultaneously assessed by global LV strains and LA volumes by 3DSTE are not associated in healthy adults. It is known that LV plays a pivotal role in maintaining circulation, as it is an ideal pump with a bullet-like shape, its walls contracting in three directions of space and its function is characterized by twisting [8,9]. Due to the Frank-Starling effect, the function of LV largely depends on its volume. If the volume of LV is increased in diastole, it stretches the LV muscles, resulting in increased contraction, which allows the LV to adapt to venous backflow, arterial demand, but without external regulation [15]. However, LV volumes are highly dependent on LA volumes as well [16]. Moreover, during the cardiac cycle, LA acts like a systolic reservoir, being a conduit in early diastole and works as a booster pump in late-diastole with special volumetric states [14,17–20]. Therefore, studying the
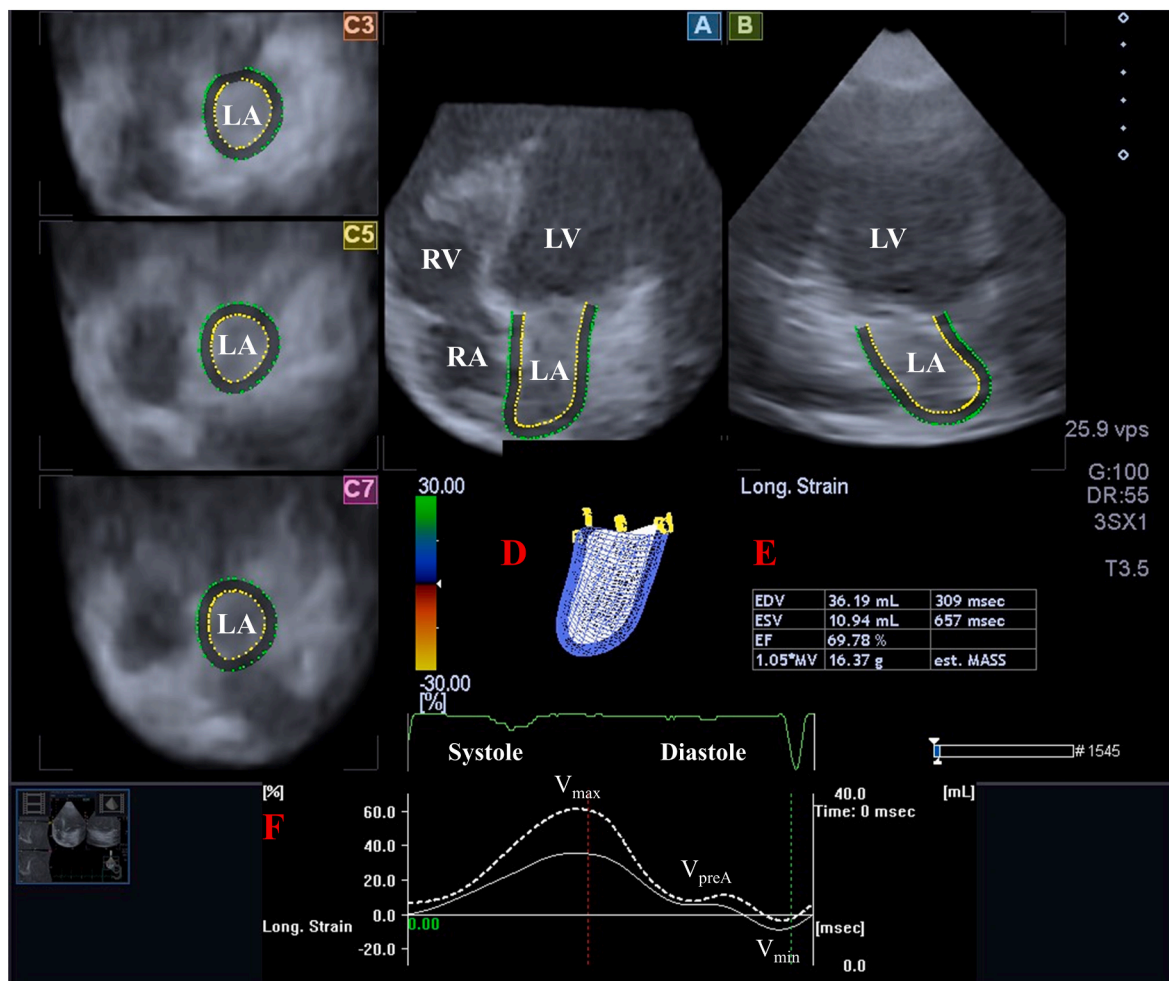
Fig. 2. Three-dimensional (3D) speckle-tracking echocardiographic analysis of left atrial (LA) volumes: apical four-chamber (A) and two-chamber (B) longitudinal views, and short-axis view at basal (C3), midatrial (C5), and superior left atrial level (C7) are shown together with a virtual 3D cast of the LA (D) and calculated LA volumetric data (E). Time – LA volume change (dashed white line) and time – LA longitudinal strain change (white line) during the cardiac cycle are also presented (F), together with maximum (Vmax), pre-atrial contraction (VpreA), and minimum (Vmin) LA volumes. **Abbreviations:** LA, left atrium; LV, left ventricle; RA, right atrium; RV, right ventricle; EDV, end-diastolic volume; ESV, end-systolic volume; EF, ejection fraction; Vmax, end-systolic maximum LA volume; VpreA, early-diastolic pre-atrial contraction LA volume; Vmin, end-diastolic minimum LA volume.

Table 1
Three-dimensional speckle-tracking echocardiography-derived left atrial volumetric and left ventricular rotational parameters.

Parameters	Measures
Left atrial volumes	
maximum left atrial volume (V_{max}, ml)	40.9 ± 13.1
pre-atrial contraction left atrial volume (V_{preA}, ml)	27.7 ± 11.8
minimum left atrial volume (V_{min}, ml)	19.4 ± 8.2
total atrial stroke volume (TASV, ml)	21.5 ± 8.2
total atrial emptying fraction (TAEF, %)	52.7 ± 11.9
passive atrial stroke volume (PASV, ml)	13.2 ± 5.6
passive atrial emptying fraction (PAEF, %)	33.3 ± 12.6
active atrial stroke volume (AASV, ml)	8.3 ± 5.8
active atrial emptying fraction (AAEF, %)	28.9 ± 11.9
Left ventricular deformation mechanics	
Left ventricular global radial strain (LV-GRS, %)	25.5 ± 9.4
Left ventricular global longitudinal strain (LV-GCS, %)	-27.6 ± 5.1
Left ventricular global circumferential strain (LV-GLS, %)	-16.2 ± 2.4
Left ventricular global three-dimensional strain (LV-G3DS, %)	28.1 ± 9.1
Left ventricular global area strain (LV-GAS, %)	-40.3 ± 5.0

relationship between LV function and LA volumes can help us understanding how they work together even in healthy circumstances.

In clinical cardiology, it is of paramount importance that all volumes and functional properties of LV and LA can be determined with quantitative characteristics, in one study, in an easy-to-learn non-invasive way. 3DSTE seems to be an ideal method to do this, as digitally collected focused 3D databases can be used to create virtual spatial models of certain heart chambers, which can be used to determine not only their volumes respecting the cardiac cycle, but contractility-features represented by strains simultaneously [1–6]. 3DSTE-derived LV strains [21–23] and LA volumes [24,25] are validated.

The results of the present study should be interpreted according to recent findings, demonstrating strong associations between LA volumes and LV rotational mechanics. These results suggest, that if during diastole a larger LA volume enters into the LV, an elevated basal LV rotation can be first detected in systole close to the mitral annulus helping emptying LV [12]. This knowledge has been extended with the present findings, that LV strains have no role in the adaptation to increased LA volumes. It is also known that if there is a larger LV volume measured in end-diastole, lower global LV-LS (and LV-AS) could be detected [7] together with preserved basal and reduced apical LV rotations [26]. Therefore, the question may well arise: what relationships can be verified between LV and LA volumes? In a recent study, strong correlations

Table 2
Left atrial volumes and global left ventricular strains in different left atrial volume groups.

	$V_{max} < 27.8$ ml (n = 24)	27.8 ml $\leq V_{max} \leq 54.0$ ml (n = 116)	54.0 ml $< V_{max}$ (n = 25)	$V_{preA} < 15.9$ ml (n = 18)	15.9 ml $\leq V_{preA} \leq 39.5$ ml (n = 124)	39.5 ml $< V_{preA}$ (n = 23)	$V_{min} < 11.2$ ml (n = 23)	11.2 ml $\leq V_{min} \leq 27.6$ ml (n = 121)	27.6 ml $< V_{min}$ (n = 21)
V_{max} (ml)	23.7±3.5	39.1±6.0*	64.9±7.1*†	25.6±5.8	38.8±8.5§	63.3±9.8‡	26.1±5.3	40.0±9.2#	61.9±11.5#&
V_{preA} (ml)	15.9±4.2	25.7±6.1*	47.6±11.4*†	12.9±2.5	25.4±5.9§	50.7±8.4§‡	14.4±3.4	26.4±7.6#	48.9±9.4#&
V_{min} (ml)	11.8±3.8	18.3±5.4*	31.3±8.9*†	9.1±1.8	18.2±4.9§	33.2±7.9§‡	9.0±1.7	18.4±4.2#	35.6±5.5#&
TASV (ml)	11.9±3.2	20.8±4.7*	33.6±7.7*†	16.5±5.0	20.6±7.0§	30.1±10.1§‡	17.0±4.6	21.4±8.0#	26.3±9.6#&
TAEF (%)	50.6±12.9	53.3±10.8	52.0±11.8	63.3±7.9	52.3±11.5§	46.9±12.3§‡	64.4±7.3	52.5±11.0#	41.4±9.7#&
PASV (ml)	7.8±3.0	13.4±4.2*	17.3±7.2*†	12.7±4.4	13.4±5.8	12.6±5.9	11.6±4.4	13.5±5.7	13.0±6.8
PAEF (%)	33.5±13.0	34.6±10.9	27.3±12.6†	48.5±8.7	33.7±11.0§	19.5±8.0§‡	43.9±11.5	33.6±11.3#	20.4±9.2#&
AASV (ml)	4.1±3.0	7.4±2.2*	16.3±8.8*†	3.8±2.0	7.2±3.4§	17.5±8.6§‡	5.4±3.2	7.9±5.6#	13.4±6.4#&
AAEF (%)	25.1±14.9	28.8±9.4	33.4±13.6*	28.3±12.9	28.1±11.3	33.9±14.2‡	34.9±14.2	28.2±11.7#	26.4±8.7#
LV-GRS (%)	27.4±10.7	25.2±7.6	25.4±7.1	28.0±11.3	25.3±9.5	25.0±8.0	26.7±7.8	25.3±10.1	25.6±7.5
LV-GCS (%)	−28.9±4.4	−27.5±5.3	−27.0±5.3	−28.3±5.0	−27.8±5.0	−26.2±5.2	−28.7±5.2	−27.6±5.1	−26.5±4.4
LV-GLS (%)	−16.2±2.2	−16.2±2.0	−16.3±2.1	−15.8±2.0	−16.3±2.5	−15.9±2.4	−16.0±2.2	−16.3±2.5	−15.8±2.5
LV-G3DS (%)	30.7±10.5	27.6±7.3	27.8±6.7	30.8±10.5	27.8±9.2	27.3±7.5	29.4±7.4	27.8±9.8	28.0±6.7
LV-GAS (%)	−41.7±4.3	−40.2±5.1	−39.8±5.6	−40.7±5.2	−40.6±4.8	−38.8±5.2	−41.1±5.4	−40.4±4.8	−39.0±5.1

Abbreviations: Vmax = left atrial maximum volume, VpreA = left atrial pre-atrial contraction volume, Vmin = left atrial minimum volume, TASV = total left atrial stroke volume, TAEF = total left atrial emptying fraction, PASV = passive left atrial stroke volume, PAEF = passive left atrial emptying fraction, AASV = active left atrial stroke volume, AAEF = active left atrial emptying fraction, LV-GRS = left ventricular global radial strain, LV-GCS = left ventricular global circumferential strain, LV-GLS = left ventricular global longitudinal strain, LV-G3DS = left ventricular global three-dimensional strain, LV-GAS = left ventricular global area strain. * $p < 0.05$ vs. Vmax < 27.8 ml, † $p < 0.05$ vs. 27.8 ml ≤ Vmax ≤ 54.0 ml, § $p < 0.05$ vs. VpreA < 15.9 ml, ‡ $p < 0.05$ vs. 15.9 ml ≤ VpreA ≤ 39.5 ml, # $p < 0.05$ vs. Vmin < 11.2 ml, & $p < 0.05$ vs. 11.2 ml ≤ Vmin ≤ 27.6 ml.

Table 3
Left atrial volumes and global left ventricular strains in different left ventricular strain groups.

	LV-GRS < 16.1 % (n = 25)	$16.1 \% \leq$ LV-GRS $\leq 34.9\%$ (n = 115)	34.9 % < LV-GRS (n = 25)	LV-GLS < -13.8% (n = 27)	$-13.8 \% \leq$ LV-GLS $\leq -18.6\%$ (n = 114)	-18.6 % < LV-GLS (n = 24)	LV-GCS < -22.5% (n = 17)	$-22.5\% \leq$ LV-GCS $\leq -32.7\%$ (n = 122)	-32.7 % < LV-GCS (n = 26)
V_{max} (ml)	39.6±9.9	41.7±13.9	37.7±11.6	43.1±14.1	40.4±13.0	39.7±12.3	42.0±11.8	41.2±13.3	37.9±12.6
V_{preA} (ml)	25.8±7.9	28.6±12.8	25.1±9.7	30.6±14.0	27.0±11.7	27.0±9.0	27.7±12.2	28.2±12.1	24.9±9.8
V_{min} (ml)	18.4±5.8	19.9±8.5	17.9±8.5	21.3±10.8	18.8±7.6	19.5±6.9	19.2±8.2	19.7±8.5	17.3±6.3
TASV (ml)	21.1±7.4	21.9±8.4	19.8±8.1	21.9±7.1	21.6±8.2	20.2±9.5	22.8±7.0	21.4±7.9	20.6±10.1
TAEF (%)	52.7±10.4	52.7±11.9	52.5±14.2	52.1±12.9	53.7±10.8	49.1±15.7	55.3±12.1	52.3±11.8	53.0±13.1
PASV (ml)	13.8±6.1	13.2±5.6	12.6±5.8	12.5±5.2	13.4±5.5	12.7±7.1	14.3±6.0	13.0±5.6	13.1±5.7
PAEF (%)	34.6±11.2	32.9±12.9	33.8±13.0	30.4±12.9	34.6±12.2	30.9±13.8	36.0±14.6	32.6±12.4	35.0±12.2
AASV (ml)	7.3±3.6	8.7±6.5	7.2±4.3	9.4±5.7	8.2±6.1	7.5±4.5	8.5±5.4	8.4±5.7	7.6±6.7
AAEF (%)	27.7±9.5	29.2±12.2	28.6±13.6	31.1±12.9	28.8±11.9	27.4±11.7	30.0±11.0	29.1±11.5	27.4±15.0
LV-GRS (%)	12.7±3.3	24.6±4.7*	42.1±6.6*†	26.8±11.6	24.6±6.6	28.4±10.3	19.4±7.2	24.6±8.3#	33.7±11.1#&
LV-GCS (%)	−25.1±4.5	−27.4±4.6*	−30.7±6.0*†	−26.2±4.5	−27.4±4.7	−30.3±6.0§	−19.8±4.2	−26.9±2.7#	−36.1±2.8#&
LV-GLS (%)	−15.6±2.1	−16.4±2.3	−16.2±3.2	−12.7±1.4	−16.3±1.3§	−20.0±1.1§	−15.7±2.3	−16.1±2.2	−17.1±3.4
LV-G3DS (%)	16.5±3.5	27.2±4.9*	43.8±6.2*†	28.8±10.5	27.2±8.3	31.5±10.6‡	21.9±7.1	27.1±7.8#	36.7±10.5#&
LV-GAS (%)	−37.8±3.9	−40.3±4.6*	−42.8±6.4*†	−36.6±4.2	−40.2±4.2§	−45.2±5.0§‡	−33.3±3.0	−40.0±3.0#	−48.0±3.6#&

Abbreviations: Vmax = left atrial maximum volume, VpreA = left atrial pre-atrial contraction volume, Vmin = left atrial minimum volume, TASV = total left atrial stroke volume, TAEF = total left atrial emptying fraction, PASV = passive left atrial stroke volume, PAEF = passive left atrial emptying fraction, AASV = active left atrial stroke volume, AAEF = active left atrial emptying fraction, LV-GRS = left ventricular global radial strain, LV-GCS = left ventricular global circumferential strain, LV-GLS = left ventricular global longitudinal strain, LV-G3DS = left ventricular global three-dimensional strain, LV-GAS = left ventricular global area strain. * $p < 0.05$ vs. LV-GRS < 16.1 %, † $p < 0.05$ vs. 16.1 % ≤ LV-GRS ≤ 34.9 %, § $p < 0.05$ vs. LV-GLS < −13.8 %, ‡ $p < 0.05$ vs. −13.8 % ≤ LV-GLS ≤ −18.6 %, # $p < 0.05$ vs. LV-GCS < −22.5 %, & $p < 0.05$ vs. −22.5 % ≤ LV-GCS ≤ −32.7%.

Table 4
Left atrial volumes and global left ventricular strains in different left ventricular strain groups.

	LV-G3DS < 19.0 % (n = 24)	19.0 % ≤ LV-G3DS ≤ 37.2 % (n = 116)	37.2 % < LV-G3DS (n = 25)	LV-GAS < -35.3 % (n = 20)	−35.3 % ≤ LV-GAS ≤ -45.3 % (n = 121)	−45.3 % < LV-GAS (n = 24)
V_{max} (ml)	39.5 ± 11.5	41.8 ± 13.5	37.1 ± 11.8	43.1 ± 12.9	41.1 ± 13.0	36.9 ± 13.1
V_{preA} (ml)	27.0 ± 10.7	28.3 ± 12.4	24.8 ± 9.8	29.7 ± 14.0	28.0 ± 11.7	23.7 ± 9.9
V_{min} (ml)	19.0 ± 7.9	19.7 ± 8.1	17.8 ± 8.5	21.4 ± 10.0	19.5 ± 8.1	16.7 ± 5.8
TASV (ml)	20.5 ± 6.7	22.1 ± 8.4	19.2 ± 8.2	21.7 ± 6.7	21.6 ± 7.9	20.2 ± 10.5
TAEF (%)	51.8 ± 10.5	53.1 ± 11.8	51.8 ± 14.2	51.5 ± 12.6	52.9 ± 11.7	53.1 ± 13.2
PASV (ml)	12.5 ± 5.4	13.5 ± 5.7	12.2 ± 5.8	13.5 ± 6.2	13.1 ± 5.6	13.2 ± 5.7
PAEF (%)	32.2 ± 11.1	33.6 ± 12.9	33.5 ± 12.9	33.2 ± 15.5	32.8 ± 12.2	36.3 ± 12.1
AASV (ml)	8.0 ± 4.4	8.6 ± 6.3	7.0 ± 4.4	8.3 ± 5.2	8.5 ± 5.7	7.1 ± 7.0
AAEF (%)	28.9 ± 10.7	29.2 ± 11.9	27.7 ± 13.8	27.5 ± 9.1	29.7 ± 11.7	26.1 ± 15.2
LV-GRS (%)	13.2 ± 4.0	24.5 ± 5.0*	22.0 ± 11.5*†	22.0 ± 11.5	24.6 ± 7.6	32.9 ± 12.4§‡
LV-GCS (%)	−25.0 ± 4.6	−27.5 ± 4.6*	−20.6 ± 2.8*†	−20.6 ± 2.8	−27.1 ± 3.0§	−36.1 ± 3.0§‡
LV-GLS (%)	−16.0 ± 2.0	−16.3 ± 2.3	−14.4 ± 2.0	−14.4 ± 2.0	−16.1 ± 2.2§	−18.2 ± 2.6§‡
LV-G3DS (%)	16.1 ± 3.1	27.1 ± 4.7*	24.5 ± 10.8*†	24.5 ± 10.8	27.1 ± 7.2	36.1 ± 11.7§‡
LV-GAS (%)	−37.9 ± 4.0	−40.3 ± 4.5*	−33.0 ± 2.2*†	−33.0 ± 2.2	−39.9 ± 2.7§	−48.8 ± 2.8§‡

Abbreviations: Vmax = left atrial maximum volume, VpreA = left atrial pre-atrial contraction volume, Vmin = left atrial minimum volume, TASV = total left atrial stroke volume, TAEF = total left atrial emptying fraction, PASV = passive left atrial stroke volume, PAEF = passive left atrial emptying fraction, AASV = active left atrial stroke volume, AAEF = active left atrial emptying fraction, LV-GRS = left ventricular global radial strain, LV-GCS = left ventricular global circumferential strain, LV-GLS = left ventricular global longitudinal strain, LV-G3DS = left ventricular global three-dimensional strain, LV-GAS = left ventricular global area strain. * $p < 0.05$ vs. LV-G3DS < 19.0 %, † $p < 0.05$ vs. 19.0 % ≤ LV-G3DS ≤ 37.2 %, § $p < 0.05$ vs. LV-GAS < −35.3 %, ‡ $p < 0.05$ vs. −35.3 % ≤ LV-GAS ≤ −45.3 %.

could be detected between LA and LV volumes and functional parameters [16]. All these findings highlight the complex relationships between LV volumes, strains and parameters characterizing rotational mechanics and LA volumes. However, further studies are warranted to examine these associations in different pathological states and disorders.

4.1. Limitation section

Several limitations have arisen as listed below:

- If we compare two-dimensional echocardiography and 3DSTE, under current technical conditions, the image quality of two-dimensional echocardiography is still better. Moreover, for adequate 3DSTE analysis, still electrocardiography gating and data acquisition within four–six heart cycles are required. The software stitches subvolumes recorded at different times to each other enables the creation of so-called stitching artifacts, which complicated the analysis. In addition, respiratory and movement artefacts and arrhythmias can make it difficult to carry out the tests [1–6].
- The overall feasibility proved to be only 55 %, which means that 45 % of healthy subjects were excluded due to inferior image quality limiting the use of 3DSTE in real-life settings. However, it should be noted, that both LV and LA had to be examined simultaneously at the same time in this study, which limited the number of cases with adequate image quality.
- Although other parameters of LV and LA can be determined in a 3DSTE study, this would have been beyond the scope of the present study.
- Similarly, other heart chambers and valves can be examined with 3DSTE, but this study did not intend to analyze this.
- In accordance with the above facts, we did not wish to validate the parameters measured with 3DSTE.
- The ventricular/atrial septum was part of the 3D LV/LA casts during the analyses. However, there can be a debate that septum is a part of which sided cardiac chamber.
- LA would have been indexed. However, purpose of this study was to assess hearts of different sizes and volumes, not individuals, therefore body mass indexation has no relevance in this case.
- Only the above mentioned examinations were performed to exclude any factors and states which could affect the findings. Any unknown factors may have influenced our results

5. Conclusions

3DSTE is suitable for simultaneous assessment of global LV strains and LA volumes. Global LV strains and LA volumes are not associated in healthy circumstances.

CRediT authorship contribution statement

Attila Nemes: Writing – original draft, Resources, Methodology, Investigation, Data curation, Conceptualization. **Árpád Kormányos:** Methodology, Investigation, Formal analysis, Data curation. **Nóra Ambrus:** Validation, Supervision. **Csaba Lengyel:** Writing – review & editing.

Declaration of competing interest

The authors declare that they have no known competing financial interests or personal relationships that could have appeared to influence the work reported in this paper.

References

[1] K.A. Ammar, T.E. Paterick, B.K. Khandheria, M.F. Jan, C. Kramer, M.M. Umland, A.J. Tercius, L. Baratta, A.J. Tajik, Myocardial mechanics: understanding and applying three-dimensional speckle tracking echocardiography in clinical practice, Echocardiography 97 (2012) 861–872.

[2] J.A. Urbano-Moral, A.R. Patel, M.S. Maron, J.A. Arias-Godinez, N.G. Pandian, Three-dimensional speckle-tracking echocardiography: methodological aspects and clinical potential, Echocardiography 29 (2012) 997–1010.

[3] D. Muraru, A. Niero, H. Rodriguez-Zanella, D. Cherata, L. Badano, Three-dimensional speckle-tracking echocardiography: Benefits and limitations of integrating myocardial mechanics with three-dimensional imaging, Cardiovasc. Diagn. Ther. 8 (2018) 101–117.

[4] L. Gao, Y. Lin, M. Ji, W. Wu, H. Li, M. Qian, L. Zhang, M. Xie, Y. Li, Clinical utility of three-dimensional speckle-tracking echocardiography in heart failure, J. Clin. Med. 11 (2022) 6307.

[5] Y. Nabeshima, Y. Seo, M. Takeuchi, A review of current trends in three-dimensional analysis of left ventricular myocardial strain, Cardiovasc. Ultrasound 18 (2020) 23.

[6] Y. Seo, T. Ishizu, A. Atsumi, R. Kawamura, K. Aonuma, Three-dimensional speckle tracking echocardiography, Circ. J. 78 (2014) 1290–1301.

[7] A. Nemes, Á. Kormányos, Z. Ruzsa, A. Achim, N. Ambrus, C. Lengyel, Complexity of left ventricular strains in response to elevated volumes in healthy adults - Detailed analysis from the three-dimensional speckle-tracking echocardiographic MAGYAR-Healthy Study, Int. J. Cardiol. Heart Vasc. 47 (2023) 101236.

[8] J.E. Hall, Guyton and Hall textbook of medical physiology, Twelfth ed., Pa, Philadelphia, 2011.

[9] S. Nakatani, Left ventricular rotation and twist: why should we learn? J. Cardiovasc. Ultrasound 19 (2011) 1–6.

[10] A. Narang, K. Addetia, An introduction to left ventricular strain, Curr. Opin. Cardiol. 33 (2018) 455–463.

[11] T. Edvardsen, L.G. Klaeboe, Imaging and heart failure: myocardial strain, Curr. Opin. Cardiol. 34 (2019) 490–494.

[12] A. Nemes, Á. Kormányos, Z. Ruzsa, A. Achim, N. Ambrus, C. Lengyel, Dependence of left ventricular rotational mechanics on left atrial volumes in non-smoker healthy adults: Analysis based on the three-dimensional speckle-tracking echocardiographic MAGYAR-Healthy Study, J. Clin. Med. 12 (2023) 1235.

[13] R.M. Lang, L.P. Badano, V. Mor-Avi, J. Afilalo, A. Armstrong, L. Ernande, F. A. Flachskampf, E. Foster, S.A. Goldstein, T. Kuznetsova, P. Lancellotti, D. Muraru, M.H. Picard, E.R. Rietzschel, L. Rudski, K.T. Spencer, W. Tsang, J.U. Voigt, Recommendations for cardiac chamber quantification by echocardiography in adults: an update from the American Society of Echocardiography and the European Association of Cardiovascular Imaging, Eur. Heart J. Cardiovasc. Imaging 16 (2015) 233–270.

[14] B.D. Hoit, Left atrial size and function: role in prognosis, J. Am. Coll. Cardiol. 63 (2014) 493–505.

[15] R. Jacob, B. Dierberger, G. Kissling, Functional significance of the Frank-Starling mechanism under physiological and pathophysiological conditions, Eur. Heart J. 13 (suppl E) (1992) 7–14.

[16] A. Nemes, Á. Kormányos, Z. Ruzsa, A. Achim, N. Ambrus, C. Lengyel, Simultaneously assessed three-dimensional speckle-tracking echocardiography-derived left ventricular and left atrial volumes are associated in healthy adults-Findings from the MAGYAR-Healthy Study, J. Clin. Med. 12 (2023) 4153.

[17] J.B. Seward, V.B. Hebl, Left atrial anatomy and physiology: echo/Doppler assessment, Curr. Opin. Cardiol. 29 (2014) 403–407.

[18] G.G. Blume, C.J. Mcleod, M.E. Barnes, J.B. Seward, P.A. Pellikka, P.M. Bastiansen, T.S.M. Tsang, Left atrial function: physiology, assessment, and clinical implications, Eur. J. Echocardiogr. 12 (2011) 421–430.

[19] L.P. Badano, A. Nour, D. Muraru, Left atrium as a dynamic three-dimensional entity: Implications for echocardiographic assessment, Rev. Esp. Cardiol. 66 (2013) 1–4.

[20] M.J. Vieira, R. Teixeira, L. Golçalves, B.J. Gersh, Left atrial mechanics: echocardiographic assessment and clinical implications, J. Am. Soc. Echocardiogr. 27 (2014) 463–478.

[21] S.A. Kleijn, W.P. Brouwer, M.F.A. Aly, I.K. Russel, G.J. de Roest, A.M. Beek, A. C. van Rossum, O. Kamp, Comparison between three-dimensional speckle-tracking echocardiography and cardiac magnetic resonance imaging for quantification of left ventricular volumes and function, Eur. Heart J. Cardiovasc. Imaging 13 (2012) 834–839.

[22] S.A. Kleijn, M.F.A. Aly, C.B. Terwee, A.C. van Rossum, O. Kamp, Reliability of left ventricular volumes and function measurements using three-dimensional speckle tracking echocardiography, Eur. Heart J. Cardiovasc. Imaging 13 (2012) 159–168.

[23] H. Ahmad, E. Gayat, C. Yodwut, M.C. Abduch, A.R. Patel, L. Weinert L, A. Desai, W. Tsang, J.G.N. Garcia, R.M. Lang, V. Mor-Avi, Evaluation of myocardial deformation in patients with sickle cell disease and preserved ejekction fraction using three-dimensional speckle tracking echocardiography, Echocardiography 29 (2012) 962–969.

[24] S.A. Kleijn, M.F. Aly, C.B. Terwee, A.C. van Rossum, O. Kamp, Comparison between direct volumetric and speckle tracking methodologies for left ventricular and left atrial chamber quantification by three-dimensional echocardiography, Am. J. Cardiol. 108 (2011) 1038–1044.

[25] M. Nagaya, M. Kawasaki, R. Tanaka, N. Onishi, N. Sato, K. Ono, T. Watanabe, S. Minatoguchi, H. Miwa, Y. Goto, T. Hirose, M. Arai, T. Noda, S. Watanabe, S. Minatoguchi, Quantitative validation of left atrial structure and function by two-dimensional and three-dimensional speckle tracking echocardiography: A comparative study with three-dimensional computed tomography, J. Cardiol. 62 (2013) 188–194.

[26] A. Nemes, Á. Kormányos, Z. Ruzsa, A. Achim, N. Ambrus, C. Lengyel, Left ventricular rotational mechanics and left ventricular volumes: is there a relationship in healthy adults?—three-dimensional speckle-tracking echocardiography-derived insights from the MAGYAR-Healthy Study, Quant. Imaging Med. Surg. 13 (2023) 6583–6589.